Resolving the acquisition ambiguity for atmospheric monitoring in multi-pass radar interferometry

Ramon Hanssen*, Dmitri Moisseev*, and Steven Businger†
*Department of Geodesy, Delft University of Technology, Delft, The Netherlands
†Department of Meteorology, University of Hawaii, Honolulu, USA
Email: hanssen@geo.tudelft.nl

***Abstract*— Atmospheric signal in spaceborne radar interferograms can be used for both meteorological interpretation in atmospheric studies, as well as for subtracting it from interferograms intended for surface deformation or topography studies. We show that atmospheric signal can be conveniently described stochastically by a power-law behavior, where the absolute amount of energy in the signal, related to the weather situation, can be described using a χ^2 probability density function, based on EUREF GPS data. We present single master stacking as well as cascaded interferogram stacking as methods to derive the atmospheric phase screen from the data.**

I. Introduction

Atmospheric monitoring using repeat-pass satellite radar interferometry enables the derivation of fine-resolution (20 m) integrated refractivity maps. Using some generally available surface pressure and temperature measurements, these maps can be converted to quantitative maps of the spatial water vapor distribution in the atmosphere [1].

The main problem in the interpretation of such maps is that they are derived from radar images acquired at different times by a process of differencing, resulting in a superposition of two atmospheric states per interferometric product. This implies that the interpretation of the atmospheric parameters suffers from the inherent acquisition ambiguity. Although distinct features in the atmospheric maps can often be attributed to one of the two acquisitions, based on the sign of the anomaly and its physical appearance, a robust separation of the effects has not been possible.

In this paper we discuss two possibilities for resolving the acquisition ambiguity and obtaining improved water vapor products. In the first approach a 'single-master' stack is used and followed by estimating the contribution of the common image by (weighted) averaging, similar to the permanent scatterers approach of Ferretti et al. [2], even though coherent distributed scattering is preferred for atmospheric applications. The second approach utilizes 'cascaded' interferograms' in which all interferometric combinations with shortest temporal baselines are computed, while the one with minimal atmospheric disturbance is used to calibrate the others. We comment on the quality of resolving the ambiguity, and what the consequences are for the derived water vapor product quality. An extension of the stochastic parameterization discussed in [3] is given based on EUREF permanent GPS observations.

II. Signal decomposition

The goal of this study is the optimal separation of the contributions of atmospheric phase delay, topography, and deformation in the observed interferometric phase. This separation is necessary whenever one of these three signals is the key parameter of interest. Regarded as a parameter estimation problem, the superposition of these signals effectively results in a rank defect. Here we will assume that a reference DEM is available with sufficient quality. Furthermore we assume that there is no unknown deformation in the region, an assumption that is valid for many areas in the world.

A. Observation statistics

The principal interferometric observation quantity is a double-difference phase measurement, where the differencing is performed both temporally and spatially. Phase observations ψ_{p,t_1} and ψ_{p,t_2} at position p and time t_i are interferometrically combined to form interferometric phase difference

$$\varphi_{p,t_1t_2} = \psi_{p,t_1} - \psi_{p,t_2}. \tag{1}$$

This temporal phase difference is not physically interpretable, due to the uncertainty in the platform and antenna phase center position, the scattering mechanisms, the phase ambiguity, and the atmospheric delays. A second spatial differencing leads to

$$\begin{aligned} \varphi_{pq,t_1t_2} &= \varphi_{p,t_1t_2} - \varphi_{q,t_1t_2} \\ &= \psi_{p,t_1} - \psi_{p,t_2} - \psi_{q,t_1} + \psi_{q,t_2} \quad \text{or} \\ \varphi &= [1,-1,-1,1]\,\psi \end{aligned} \tag{2}$$

for short, with variance-covariance (vc) matrix

$$Q_\psi = \begin{bmatrix} \sigma^2_{p,1} & \sigma_{p,12} & & \\ \sigma_{p,12} & \sigma^2_{p,2} & & \\ & & \sigma^2_{q,1} & \sigma_{q,12} \\ & & \sigma_{q,12} & \sigma^2_{q,2} \end{bmatrix}. \tag{3}$$

In this representation we assume no correlation between observations at position p and q, that is, we assume spatially correlated atmospheric signal as an unknown parameter to be estimated, not as noise. The phase observations ψ_{p,t_i} depend on the physical interaction of the radar waves with the earth's surface, which is generally inpredictable for distributed scattering mechanisms. As a result, the probability density function (pdf) of the phase observation is uniform in the $[-\pi,+\pi)$ interval, and zero elsewhere. This results

in a variance of $\sigma_p^2 = \sigma_q^2 = \pi^2/3$. The existence of non-zero covariance terms $\sigma_{p,12}$ are the key to the application of interferometry. Assuming that the scattering mechanisms, driven by the physical distribution of scatterers on earth and the interferometric geometry, are correlated causes relatively large covariance values which decrease the variance of the double-difference interferometric observables ϕ.

Although the variance terms in Q_ψ are known from the uniform phase distribution, using a set of two radar acquisitions to form an interferogram does not give a reliable estimate of the covariance terms. Conventional methods assume ergodicity and use a spatial window to estimate the covariance per point, or its equivalent parameter coherence. This methodology obviously fails whenever the ergodicity assumption is incorrect, in the case of inhomogeneous scattering mechanisms. Using a multitude of radar acquisitions over a specific area a temporal coherence can be derived, which is available on a pixel-by-pixel basis.

B. Parameters of estimation

The three unknown parameters atmosphere, topography, and deformation can be distinguished using there temporal and spatial characteristics and their dependence on the perpendicular baseline. Topography is independent in time and scales linearly with the perpendicular baseline of the interferometric combinations. Spatial correlation exists in a degree dependent on the expected roughness of the topography. Deformation is usually temporall and spatially correlated. In time, deformation can usually be estimated in a first order analysis as a linear process. Higher order deformation terms might be estimated in an iterative approach, depending on the quantity and quality of observations. Deformation is independent of the perpendicular baseline, but usually spatially correlated. Atmospheric signal is spatially correlated following a power law behavior, temporally uncorrelated over intervals of one or more days, while the signal is the superposition of two atmospheric states related to the two acquisitions, indicated as the acquisition ambiguity.

III. Tropospheric variability

Atmospheric signal in the radar interferograms manifests itself as a double-difference of slant-integrated refractivity: spatial variability within a radar scene is differenced between two acquisitions. This implies that the total delay signal, regarded as a mean value and variability around that mean, cannot be measured. Previous studies have shown that atmospheric signal exhibits a scaling behavior—the energy contained at specific spatial scales is exponentially related to the energy at different scales:

$$\begin{aligned} P_a(f) &= P_0(f/f_0)^{-\beta}, \quad \text{or linearly in loglog:} \\ \ln P_a(f) &= -\beta \ln f + (\ln P_0 - \ln f_0) \end{aligned} \tag{4}$$

where f is the spatial wavenumber, P_0 and f_0 are normalizing constants, and $-\beta$ is the spectral index. Alternatively, this relation can be expressed by the structure function, covariance function, or 2D fractal dimension. All three expressions are valid within a limited range of scales due to physical restrictions.

A. Relative variability

Based on atmosphere-only, 1-day interval interferograms over relatively flat areas, it has been shown [3] that atmospheric signal exhibits a scaling behavior in two distinct regimes. For spatial scales less than the effective turbulent tropospheric thickness, say 2-5 km, the spectral index is close to $-8/3$, whereas for larger scales up to the interferogram sizes the spectral index decays to $-5/3$ and smaller. In fact, due to the removal of nearly linear trends induced by orbit errors the spectral index flattens over long distances. Thus we have

$$P_a(f) = \begin{cases} P_0(f/f_0)^{-8/3} & \text{for } 0 \le (f_0/f) < 3 \text{ km}, \\ P_0\,(f_0/3)\,(f/f_0)^{-5/3} & \text{for } 3 \le (f_0/f) < 50 \text{ km}, \end{cases} \tag{5}$$

These observations correspond with Kolmogorov turbulence theory, which expects a spectral index of $-5/3$ moving in any direction in a three-dimensional turbulent volume. Vertical integration of refractivity results in an atmospheric phase screen with a spectral index of $-8/3$. Here it is assumed that the horizontal spatial scales are less than the finite physical height of the turbulent medium, which relates to a 3D volume. Moving to larger scales, the medium becomes relatively more and more flat, effectively a thin, nearly 2D slice. For these scales the roughness increases, resulting in the $-5/3$ regime. For larger distances, further flattening of the spectra is expected.

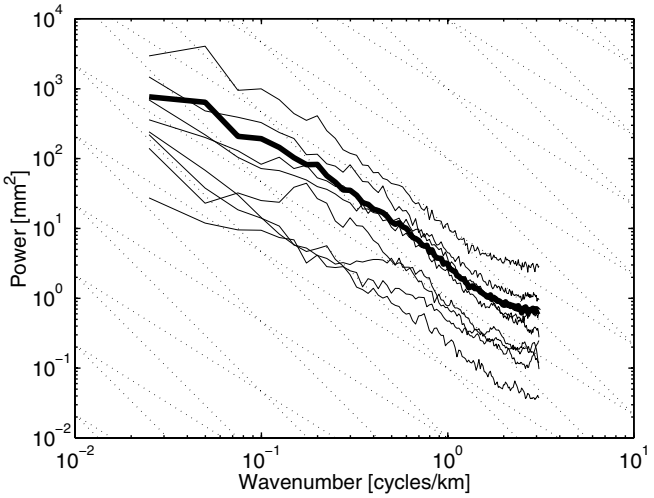

Fig. 1. Power spectra of atmospheric signal in eight independent interferograms. Diagonal lines indicate -5/3 and -8/3 power slopes. The bold line reflects the average spectrum.

Fig. 1 illustrates the hypothesis of a scaling behavior over two regimes. Independent atmospheric interferograms over an area in the Netherlands were used to obtain these observations. The flattening of the spectra at high wavenumbers is due to noise in the observations. The vertical position of these spectra is indicative for the amount of energy during that specific interferogram which is directly related to the instability of

the boundary layer. It is important to note that the energy in the atmospheric signal varies over more than one order of magnitude. As a result, the lowest spectrum in fig. 1 corresponds with a nearly flat atmospheric phase screen. We will use this property in section IV-B.

B. Absolute variability

The (relative) scaling behavior of atmospheric signal as a function of distance is an elegant way for modeling or simulating an atmospheric phase screen for a radar acquisition. Nevertheless, the absolute amount of variability, expressed by the P_0 coefficient, is necessary to obtain realistic values. For a specific location, it is important to know the likelihood of a specific value of the P_0 coefficient. Since this is not readily available for these high spatial resolutions and accuracy, we used Zenith Total Delay variability derived from permanent GPS receivers of 138 EUREF stations over the year 2002. Hourly ZTD values were recorded with a mean standard deviation of 3.3 mm [4].

We assume that a specific weather situation can be expressed by analyzing the variability of ZTD per day, using 24 measurements. This yields over 365 days of variances, which are related to instable, convective weather with much water vapor (high variances) or stable weather situations without much refractivity changes. Expressing these variances in a histogram gives an indication for the likelihood of a particular weather situation, parameterized by the delay variability. It is evident that the amount of variability during a full day is larger than during only a few hours, comparable with a spatial snapshot in an interferogram. Moreover, the GPS observations do not reflect the small changes within the hourly sampling and use zenith averaging using satellites distributed over a wide part of the sky. Nevertheless, we assume that the obtained variances are a scaled version of the variability within a shorter time frame and over smaller spatial scales. Under this assumption, the abundance of data in the EUREF network allows for deriving the necessary statistics.

Figure 2 shows the histograms of the daily ZTD variability. For 114 stations with over 300 days of hourly observations, the histograms are shown in gray values. The average histogram is indicated by the bold black line. A best-fit χ^2 distribution is found for 2 degrees of freedom and a non-centrality parameter of 10, and indicated by the dashed line. The maximum likelihood value for daily ZTD variability is to be a standard deviation of 8 mm. Assuming that the distributions reflect the likelihood of a specific weather situation (in terms of electromagnetic wave propagation), it is interesting to observe that most stations show the same type of behavior. A standard deviation of 3–4 cm or more has only a small likelihood, whereas most of the variability seems to be in the range 2 mm to 2 cm.

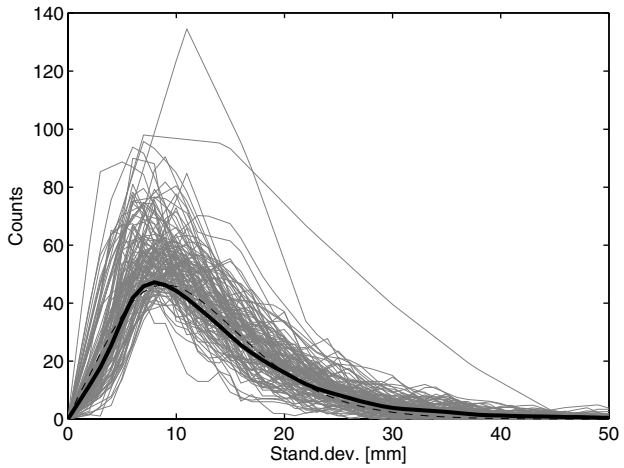

Fig. 2. Histograms of daily atmospheric delay variability (standard deviation) for 114 EUREF stations. The bold black line is the average distribution, and the dashed line shows a best-fit χ^2 distribution.

IV. Stacking approaches

The atmospheric acquisition ambiguity hampers the interpretation of the atmospheric signal per acquisition. The availability of a multitude of images enables two stacking methodologies to estimate the atmospheric phase screen per acquisition. The 'single-master' approach, fig. 3B, is convenient for deformation monitoring and can be applied in a permanent scatterers approach or over areas which remain coherent over many years. However, most natural areas decorrelate as a function of time. Therefore, it would be advantageous to use interferometric combinations with a temporal baseline as small as possible, shown in fig. 3A and termed as 'cascaded' interferograms.

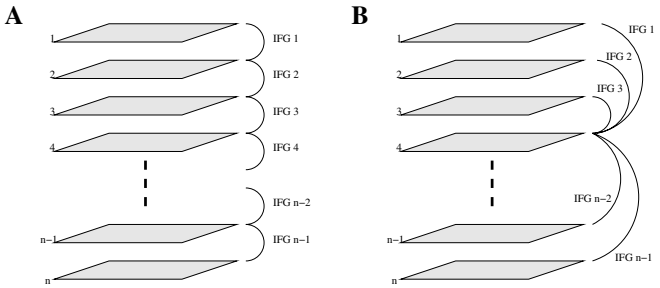

Fig. 3. Two stacking approaches. **A)**'Cascaded' interferograms: every SAR image appears in two interferograms, except the first and last, and **B)** 'single master' stack, where every interferogram refers to the same master image.

A. Single master stacking

For n radar acquisitions the single-master stack is obtained from

$$\begin{bmatrix} i_1 \\ \vdots \\ i_{n-1} \end{bmatrix} = \begin{bmatrix} -I_{k-1} & [1]_{k-1} & 0 \\ & & \\ 0 & [1]_{n-k} & -I_{n-k} \end{bmatrix} \begin{bmatrix} a_1 \\ \vdots \\ a_n \end{bmatrix} \qquad (6)$$

where acquisition k is used as reference (master) image, I_i is the unit matrix with dimension 1, $[1]_{k-1}$ is a vector of ones. The interferogram variance-covariance matrix is now

$$Q_i = \sigma_a^2 \begin{bmatrix} 2 & 1 & \dots & 1 \\ 1 & \ddots & \ddots & 1 \\ \vdots & \ddots & \ddots & 1 \\ 1 & \dots & 1 & 2 \end{bmatrix} \tag{7}$$

Taking the (unweighted) sum of all interferograms yields

$$\frac{1}{n-1}\left[1,1,\dots,1\right]\begin{bmatrix} i_1 \\ \vdots \\ i_{n-1} \end{bmatrix} = a_k - \frac{1}{n-1}\sum_{l=1}^{n\backslash k} a_l \quad \text{or}$$
$$\frac{1}{n-1}\sum_{l=1}^{n-1} i_l = a_k + \varepsilon \tag{8}$$

with $E\{\varepsilon\} = 0$ and $D\{\varepsilon\} = \frac{\sigma_a^2}{n-1}$ this yields the estimate for the APS of the master image

$$\hat{a}_k = \frac{1}{n-1}\sum_{l=1}^{n-1} i_l \quad \text{with precision}$$
$$\sigma_{\hat{a}_k}^2 = \frac{\sigma_a^2}{n-1} \tag{9}$$

where σ_a^2 is the atmospheric variance per acquisition.

B. Cascaded interferogram stacking

Whereas the single-master approach estimates the master APS using a rigourous (weighted) averaging, experience shows that in a time series of radar interferograms there are always interferograms which show a negligible APS variability. The lowest spectrum in fig. 1 is an example of such a situation. Usually these situations occur during cold and stable weather situation, where the water vapor content is low. The idea behind the cascaded stack is to use this information and find the interferogram with minimal variance. The cascade stack is obtained from

$$\begin{bmatrix} i_1 \\ \vdots \\ i_{n-1} \end{bmatrix} = \begin{bmatrix} 1 & -1 & & \\ & \ddots & \ddots & \\ & & 1 & -1 \end{bmatrix} \begin{bmatrix} a_1 \\ \vdots \\ a_n \end{bmatrix} \tag{10}$$

with vc-matrix

$$Q_i = \sigma_a^2 \begin{bmatrix} 2 & -1 & 0 & 0 \\ -1 & 2 & \ddots & 0 \\ 0 & \ddots & \ddots & -1 \\ 0 & 0 & -1 & 2 \end{bmatrix}. \tag{11}$$

After finding the interferogram with minimal phase variance, say, interferogram k with $i_k = a_k - a_{k+1}$ we simply pose that the expectation values $E\{a_k\} = E\{a_{k+1}\} = 0$ and $D\{a_k\} = D\{a_{k+1}\} = \sigma_{i_k}^2$, the observed variance $\sigma_{i_k}^2$. Thus, we overestimate the true variance of a_k and we can regard this as an upper bound on the variance. Retrieving the APS per acquisition

$$\begin{bmatrix} a_1 \\ a_2 \\ \vdots \\ a_{k-1} \\ a_{k+2} \\ \vdots \\ a_n \end{bmatrix} = \begin{bmatrix} 1 & 1 & \dots & 1 & & & \\ & 1 & & 1 & & & \\ & & & 1 & & & \\ & & & & -1 & & \\ & & & & -1 & -1 & \\ & & & & -1 & \dots & -1 \end{bmatrix} \cdot \begin{bmatrix} i_1 \\ i_2 \\ \vdots \\ i_{n-1} \end{bmatrix}. \tag{12}$$

with vc-matrix

$$Q_a = \sigma_{i_k}^2 \, I_{n-2} \tag{13}$$

This approach has the advantage over the single-master stack that the error can be 'chosen' opportunistically, since the error budget is fully determined by the interferogram with minimal phase variation. This is especially efficient for scaling signals which have orders of magnitude variation in energy. In contrast, single master stacking, especially in its unweighted form, minimizes the variance of the master atmospheric phase screen by averaging, see eq. (9). This implies that (i) sufficient acquisitions need to be available, and (ii) the presence of a coincidental 'perfect' interferogram is not used. It needs to be noted that by weighting the single-master stack, comparable results can be obtained

V. Conclusion

Atmospheric signal in radar interferograms can be used for both meteorological interpretation in atmospheric studies, as well as for subtracting it from interferograms intended for surface deformation or topography studies. We have shown that atmospheric signal can be conveniently described stochastically by its power-law behavior. The absolute amount of energy in the signal, related to the weather situation, can be described using a χ^2 probability density function, based on EUREF GPS stations. We presented single master stacking as well as cascaded interferogram stacking as methods to derive atmospheric phase screen from the data.

Acknowledgment

The authors would like to thank the European Space Agency for supporting this study.

References

[1] R. F. Hanssen, T. M. Weckwerth, H. A. Zebker, and R. Klees, "High-resolution water vapor mapping from interferometric radar measurements," *Science*, vol. 283, pp. 1295–1297, 1999.

[2] A. Ferretti, C. Prati, and F. Rocca, "Nonlinear subsidence rate estimation using permanent scatterers in differential SAR interferometry," *IEEE Transactions on Geoscience and Remote Sensing*, vol. 38, no. 5, pp. 2202–2212, Sept. 2000.

[3] R. F. Hanssen, *Radar Interferometry: Data Interpretation and Error Analysis*. Dordrecht: Kluwer Academic Publishers, 2001.

[4] W. Soehne and G. Weber, "Epn special project "troposphere parameter estimation"," in *EUREF Symposium, Ponta Delgada, Portugal, June 2002*, 2003, pp. 1–6.